Bulletin of the Seismological Society of America, Vol. 99, No. 6, pp. 3516–3524, December 2009, doi: 10.1785/0120090062

Short Note

Intrinsic and Scattering Q near 1 Hz across the East African Plateau

by Alemayehu L. Jemberie and Andrew A. Nyblade

Abstract Crustal attenuation across the East African plateau in Tanzania, an area of uplifted and rifted Precambrian crust, has been investigated using seismic data from regional earthquakes recorded by the 1994–1995 Tanzania broadband seismic experiment. We use 1 Hz *Lg* coda waves from the 17 events, together with the energy flux model of Frankel and Wennerberg (1987), to obtain estimates of intrinsic (Q_I) and scattering (Q_S) attenuation for East Africa. Q_I values across the plateau are fairly uniform, ranging from a low of ~300 to a high of ~600. Q_I values for the Tanzania craton, in the middle of the plateau, are similar to those for the mobile belts, which form the sides of the plateau. Q_I of 300 to 600 is somewhat lower than the average crustal Q for Precambrian terrains elsewhere. Heat flow from the Tanzania craton and surrounding mobile belts is not elevated; therefore, we attribute the lower-than-average Q values not to elevated crustal temperatures, but instead to rift faults in the crust that are interconnected and filled with fluids. Q_S ranges from ~1000 in the mobile belts and along the eastern margin of the Tanzania craton to ~2200 in the north central part of the plateau just south of Lake Victoria. We attribute the variability in Q_S to scattering of *Lg* by surface topography, in particular, rift basins along the eastern side of the plateau.

Introduction

The attenuation of seismic waves by crustal structure has long been recognized as a first-order seismological phenomenon, yet its causes are still debated. For example, intrinsic attenuation (Q_I) has been attributed to fluid-filled interconnected cracks in the crust in some studies (e.g., O'Connell and Budiansky, 1977; Mitchell, 1995), but to elevated temperatures in others (e.g., Frankel *et al.*, 1990; Frankel, 1991; Baumont *et al.*, 1999; Sarker and Abers, 1999; Fan and Lay, 2003; Xie *et al.*, 2004; Hauksson and Shearer, 2006; Zor *et al.*, 2007). In support of the latter interpretation, it has been shown that in some areas Q_I decreases with increasing heat flow (e.g., Zor *et al.*, 2007), while in support of the former interpretation, it has been shown that regional differences in Q_I can be correlated with variations in the volume of fluids in the crust (e.g., Mitchell, 1995; Mitchell *et al.*, 2008). In contrast to Q_I, scattering attenuation (Q_S) appears to be better understood, arising from the scattering of seismic energy by irregular topography, complex surface geology, and heterogeneous structure within the crust (Aki, 1969).

In this article, we investigate crustal attenuation across the middle of the East African plateau in Tanzania, an area of Precambrian crust that has been uplifted into a broad plateau and affected by Cenozoic rift faulting. By using 1 Hz *Lg* coda waves and the energy flux model of Frankel and Wennerberg (1987), we make estimates of Q_I and Q_S, providing the first such estimates for East Africa. We then combine our Q estimates with ancillary information on heat flow, crustal structure, and topography to gain further insights into the factors affecting crustal attenuation. Results from this article will also be useful for future seismic investigations that require corrections for path and site effects on seismic amplitudes, in particular, investigations involving seismic source scaling and magnitude estimation.

Background

The Precambrian tectonic framework of the East African plateau consists of the Archean Tanzania craton surrounded by the Proterozoic Kibaran, Ubendian, and Mozambique belts (Fig. 1). The Cenozoic East African Rift System (EARS) has developed primarily within the mobile belts around the craton forming two branches, eastern and western (Fig. 1). The eastern branch begins at the Afar triple junction and continues south through west-central Kenya and into northern Tanzania, transecting the northeast corner of the East African plateau. The eastern branch formed primarily within the Mozambique belt, but in northern Tanzania it impinges on the eastern margin of the craton, where rift faults penetrate up to 100–200 km into the interior of the craton, fracturing the craton margin into many fault blocks (Fig. 1).

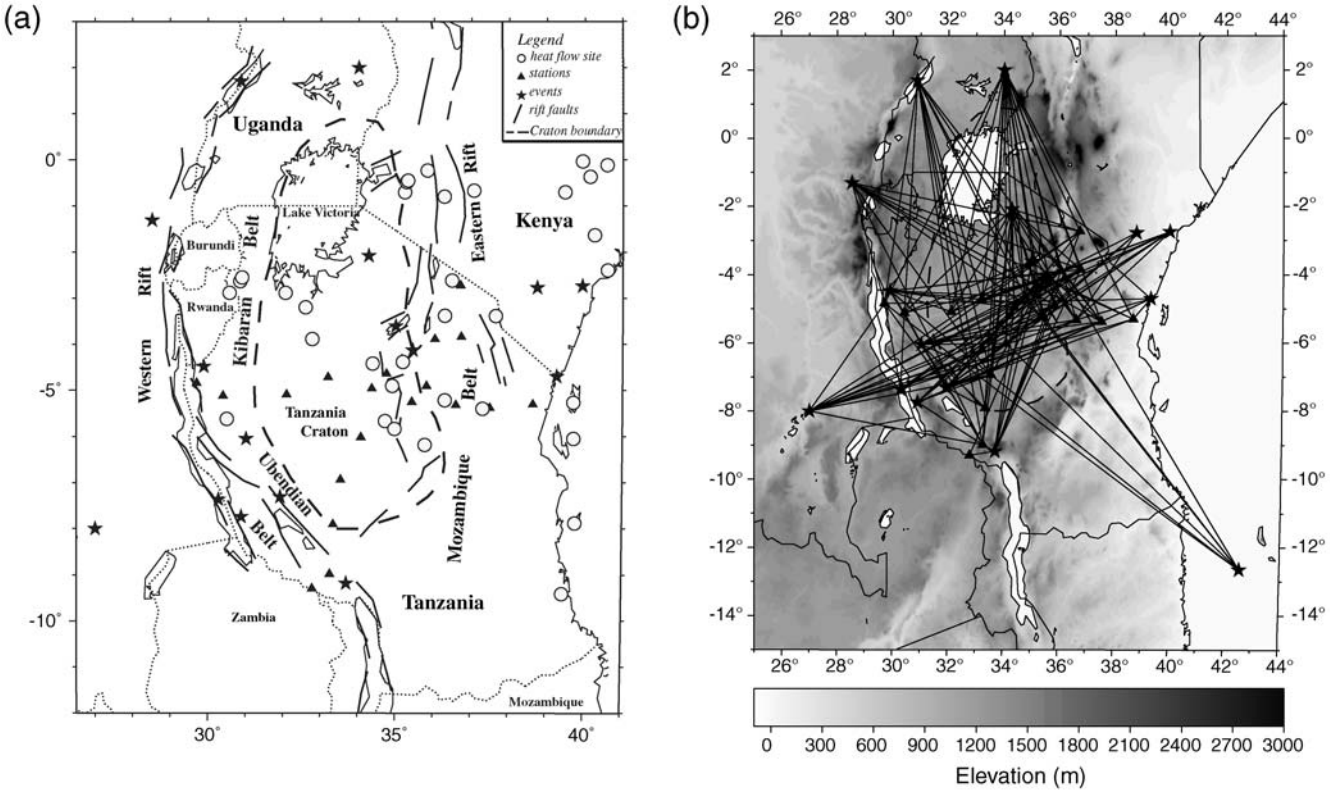

Figure 1. (a) Map showing political boundaries (dotted lines), outline of the Tanzania craton (dashed line), mobile belts, fault lines (bold lines), earthquakes used in this article (solid stars), stations from the 1994–1995 Tanzania broadband seismic experiment (solid triangles), and location of heat flow measurements (open circles) from Nyblade *et al.* (1990) and Nyblade (1997). (b) Gray-shaded elevation map showing event-station path coverage. Event locations are shown with solid stars and seismic stations with solid triangles. The bold dashed line shows the location of the Tanzania craton.

The western branch of the EARS defines the western side of the East African plateau (Fig. 1); some of the deepest rift lakes have formed within the many rift valleys that comprise the western branch.

Early studies of crustal structure in East Africa used seismic refraction data and observations from teleseismic and regional earthquakes to image the crust (Bonjer *et al.*, 1970; Griffiths *et al.*, 1971; Long *et al.*, 1972; Mueller and Bonjer, 1973; Bram and Schmeling, 1975; Nolet and Mueller, 1982; Hebert and Langston, 1985). These studies yielded estimates of Moho depths of 40 to 48 km beneath unrifted crust and of 20 to 32 km under the rift valleys. Investigations of crustal structure in and around the Kenya rift using refraction profiling were undertaken by the Kenya Rift International Seismic Project (KRISP) (Prodehl *et al.*, 1994; Fuchs *et al.*, 1997 and references therein). The KRISP group found that along the axis of the Kenya rift Moho depths shallow northward from 32 km at the equator to ~20 km beneath Lake Turkana. Away from the rift, they obtained crustal thicknesses of 34 to 40 km beneath the Tanzania craton and 35 to 42 km beneath the Mozambique belt.

More recent investigations of crustal structure in East Africa by Last *et al.* (1997), Dugda *et al.* (2005), and Julia *et al.* (2005) using teleseismic receiver functions and Rayleigh wave dispersion measurements, and Langston *et al.* (2002) using regional waveforms, have provided additional information about crustal structure in the mobile belts and Tanzania craton. For the Tanzania craton, Mozambique belt, and Ubendian belt, Moho depths range from 37 to 42 km, 36 to 39 km, and 40 to 45 km, respectively, typical of Precambrian crust elsewhere (e.g., Rudnick and Gao, 2004). Thus, outside of the rift valleys proper, crustal thickness across the East African plateau appears to be largely unperturbed by the Cenozoic rifting (Dugda *et al.*, 2005).

Data for this article come from the 1994–1995 Tanzania broadband seismic experiment. This experiment consisted of 20 broadband seismographs deployed in two 1000 km long arrays crossing the plateau from west to east and from southwest to northeast (Fig. 1). Station spacing varied between 50 and 200 km. Nine of the seismic stations were located within the Tanzania craton, seven stations were in the Mozambique belt, and four stations were in the Ubendian belt (Fig. 1). Additional details of the field deployment are given by Nyblade *et al.* (1996). Preliminary locations and magnitudes for some 2500 local and regional earthquakes recorded by the experiment are reported in Langston *et al.* (1998).

Method

Intrinsic and scattering attenuation can be estimated from the *Lg* wave and its coda on transverse component seismograms at local and regional distances. The *Lg* wave is a crustal guided wave (Kennett, 1986; Langston et al, 2002); hence, it is affected by crustal attenuation. Typically, the *Lg* wave is the largest amplitude wave within the seismic wave train recorded in continental settings at local and regional distances. The *Lg* wave travels with a group velocity between 3.2 and 3.6 km/sec (Press and Ewing, 1952; Kennett, 1986), and is recorded on both vertical and transverse component seismograms. It can be modeled either as a superposition of many higher mode surface waves trapped in the crust (Kennett, 1986; Langston *et al.*, 2002), or as the interference of supercritically reflected *S* waves, bouncing up and down between the Moho and the free surface (Kennett, 1986; Langston *et al.*, 2002).

Over 200 local and regional earthquakes with magnitudes greater than 2.0 recorded by the Tanzania broadband seismic experiment and reported in the event catalog of Langston *et al.* (1998) were examined. After removing the instrument effect from the seismograms, the north–south and east–west components were rotated into radial and transverse components. The quality of the *Lg* wave on each transverse component seismogram was inspected and compared to the background noise. Seismograms from earthquakes with magnitudes less than 2.8, as well as many from earthquakes with magnitudes between 2.8 and 3.8, were found to have poor signal to noise ratios and could not be used. Only 17 events had sufficiently high quality waveforms for use in our analysis (Table 1; Figs. 1a,b). Fortunately, these events are spread throughout the East African plateau, providing adequate *Lg* path coverage to characterize Q across the center of the plateau (Fig. 1b).

The two-dimensional energy flux model of Frankel and Wennerberg (1987) was applied to estimate Q_I and Q_S using the *Lg* wave coda, following the method of Jemberie and Langston (2005), along with an *Lg* group velocity of 3.5 km/sec taken from Langston *et al.* (2002). Using the *Lg* wave coda has advantages over using just the *Lg* wave for estimating both Q_I and Q_S, as discussed by Frankel and Wennerberg (1987). A brief review of the method for estimating Q_I and Q_S using the energy flux model is provided.

The envelope of the seismic coda is very stable and independent of source-station distance. The level of the coda envelope is controlled by scattering attenuation while its slope is controlled by intrinsic attenuation (Frankel and Wennerberg, 1987; Jemberie and Langston 2005). The higher the scattering attenuation, the higher the level of the coda will be and vice versa. The higher the intrinsic attenuation, the lower the slope of the code will be and vice versa. The envelope amplitude for a two-dimensional energy flux model is given by:

$$A_c = \sqrt{2I_d}\, t_d^{1/2} t^{-1} e^{-\omega t/(2Q_I)} e^{\omega t_d (1/Q_I + 1/Q_s)/2} \sqrt{1 - e^{-\omega t/Q_s}}, \quad (1)$$

where I_d is the integral of the square of the direct wave seismogram amplitude. t_d and t are the direct wave arrival time and coda lapse time in seconds, respectively, measured from the earthquake origin time. Q_I is intrinsic Q and Q_S is scattering Q. ω is the angular frequency measured in radians/sec.

Q_I and Q_S with ± 1 standard deviations were calculated by a least-square inversion of the observed coda amplitude. The coda amplitude between $2t_d$ and the beginning of the noise level is used in the determination of the Q values (e.g., Jemberie and Langston, 2005). Figure 2 a illustrates the process of determining the normalizing factor $\sqrt{I_d}$ in

Table 1
List of Earthquakes Recorded Used in This Article

Event	Longitude (°)	Latitude (°)	Magnitude	Origin Time (UTC*) (hr:min:sec)	Origin Date (dd/mm/yyyy)
1	28.5161	−1.3104	5.0	11:50:53.0	29/04/1995
2	27.0000	−8.0000	5.0	11:50:15.0	29/04/1995
3	42.5439	−12.6499	4.7	02:32:20.0	27/04/1995
4	38.7280	−2.7730	3.2	17:25:03.0	07/04/1995
5	39.9300	−2.7400	4.6	12:22:49.0	27/02/1995
6	30.2760	−7.3610	4.2	00:40:04.0	12/12/1994
7	34.9830	−3.6030	4.0	08:09:22.0	02/12/1994
8	29.8900	−4.4780	4.2	04:06:03.0	19/11/1994
9	33.6790	−9.1810	4.5	01:08:07.0	16/11/1994
10	34.2600	−2.0800	4.1	04:09:42.0	07/10/1994
11	31.0100	−6.0460	4.4	01:36:59.0	30/09/1994
12	30.8815	−7.7378	4.6	04:08:50.0	05/09/1994
13	30.8760	1.7050	4.9	14:59:58.0	31/08/1994
14	34.0000	2.0000	4.3	19:56:39.0	22/08/1994
15	31.751	−7.433	6.0	00:45:47.0	18/08/1994
16	35.4300	−4.1300	3.8	11:32:11.0	20/07/1994
17	39.2520	−4.7030	2.8	09:11:04.0	07/06/1994

*Coordinated Universal Time.

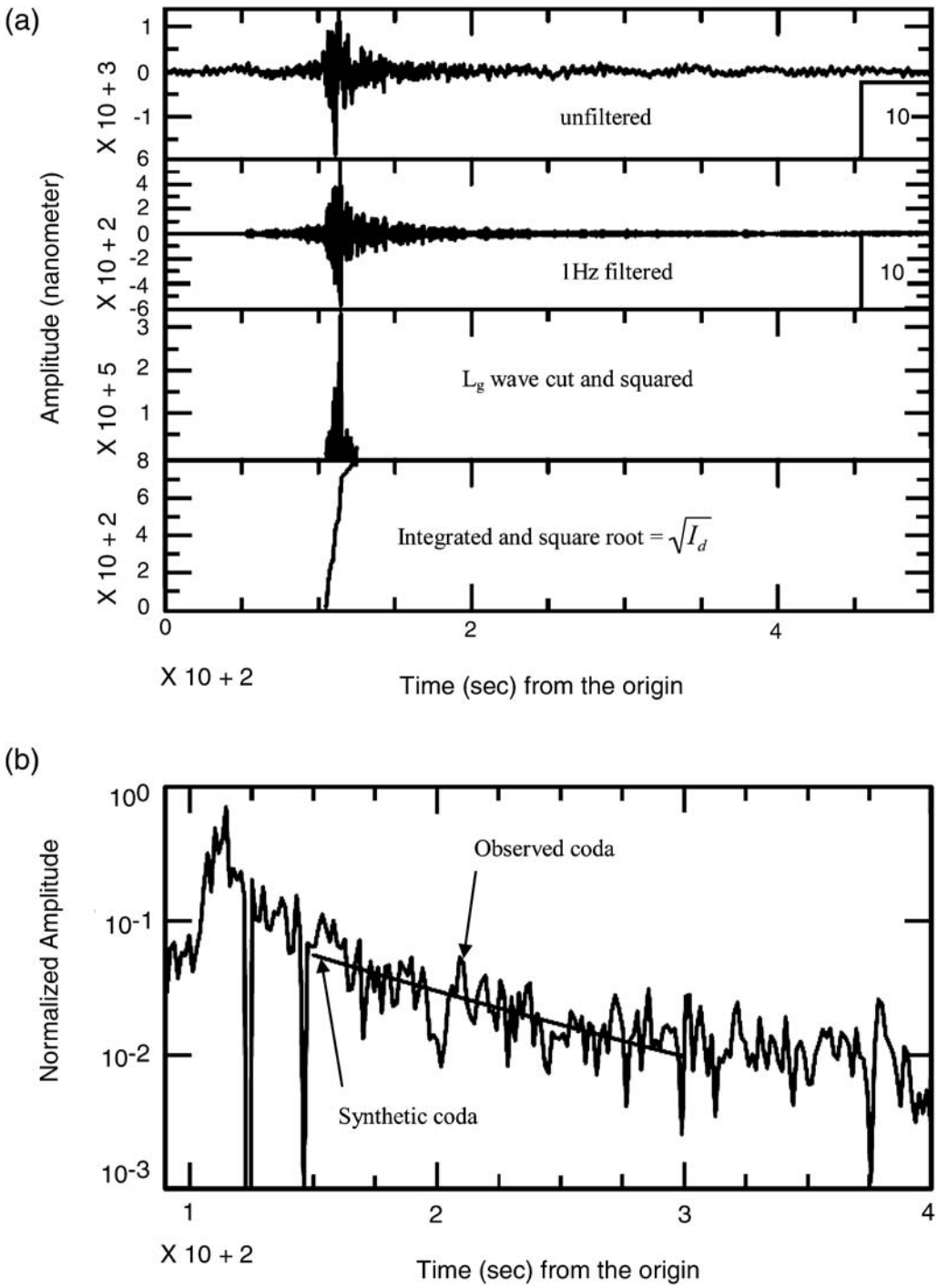

Figure 2. (a) Steps in calculating the normalization factor $\sqrt{I_d}$ for event number 8 (Table 1) recorded by station URAM (Latitude = −5.0878, Longitude = 32.0832). The instrument corrected transverse component is band-passed around 1 Hz. The primary arrival (L_g) is isolated (cut) and squared. The square root of the integral of the squared L_g gives $\sqrt{I_d}$. (b) The envelope of the normalized (with respect to $\sqrt{I_d}$) 1 Hz observed coda and synthetic coda.

equation (1). A second order Butterworth band-pass filter with corner frequencies ±10% of the center frequency (1 Hz) was applied to each transverse component. The primary arrival of the filtered seismogram is cut, squared, integrated, and the square root of the integral is computed to obtain $\sqrt{I_d}$. The envelope of the observed coda is computed from the filtered and normalized (with respect to $\sqrt{I_d}$) seismogram by calculating the amplitude of the analytical signal (Farnbach, 1975). The coda is normalized by $\sqrt{I_d}$ to remove the effects of possible site amplifications from the amplitude of the *Lg* coda (Jemberie and Langston, 2005). The logarithm of the normalized form of equation (1) was then fit

to the logarithm of the normalized observed coda envelope using a least-square algorithm (Fig. 2b) to get Q_I and Q_S.

Results and Discussion

Coda is formed by scattered energy from inhomogeneous structure near Earth's surface within an expanding ellipsoid whose foci are given by the location of the earthquake source and recording station (Aki, 1969; Sato, 1977).

However, in equation (1) the normalization factor $\sqrt{I_d}$ is obtained from the direct Lg wave, which is predominantly sensitive to Q and velocity structure along the path between the earthquake hypocenter and the recording station. Therefore, to estimate lateral variations in Q, we use the procedure outlined in Jemberie and Mitchell (2004) in which each path is divided into 10 equal segments; at the beginning and end of each segment the Q value for that path is assigned. Whenever two or more event-station paths cross at a point, the average of the Q values for the paths is assigned at the intersection. The assigned Q values are then contoured using the contouring algorithm in the Generic Mapping Tool (GMT) (Wessel and Smith, 1998) to produce smoothed maps showing Q variations across the study area (Figs. 3a,b). In other recent studies (e.g., Mayeda *et al.*, 2005; Morasca *et al.*, 2008), coda amplitude measurements also have been inverted for event-station path Q, assuming that the early part of the coda behaves as if it were a direct wave.

Q_I values over the study area are fairly uniform, ranging from a low of ~300 to a high of ~600. Similar values of Q_I are found in both the Tanzania craton and the surrounding

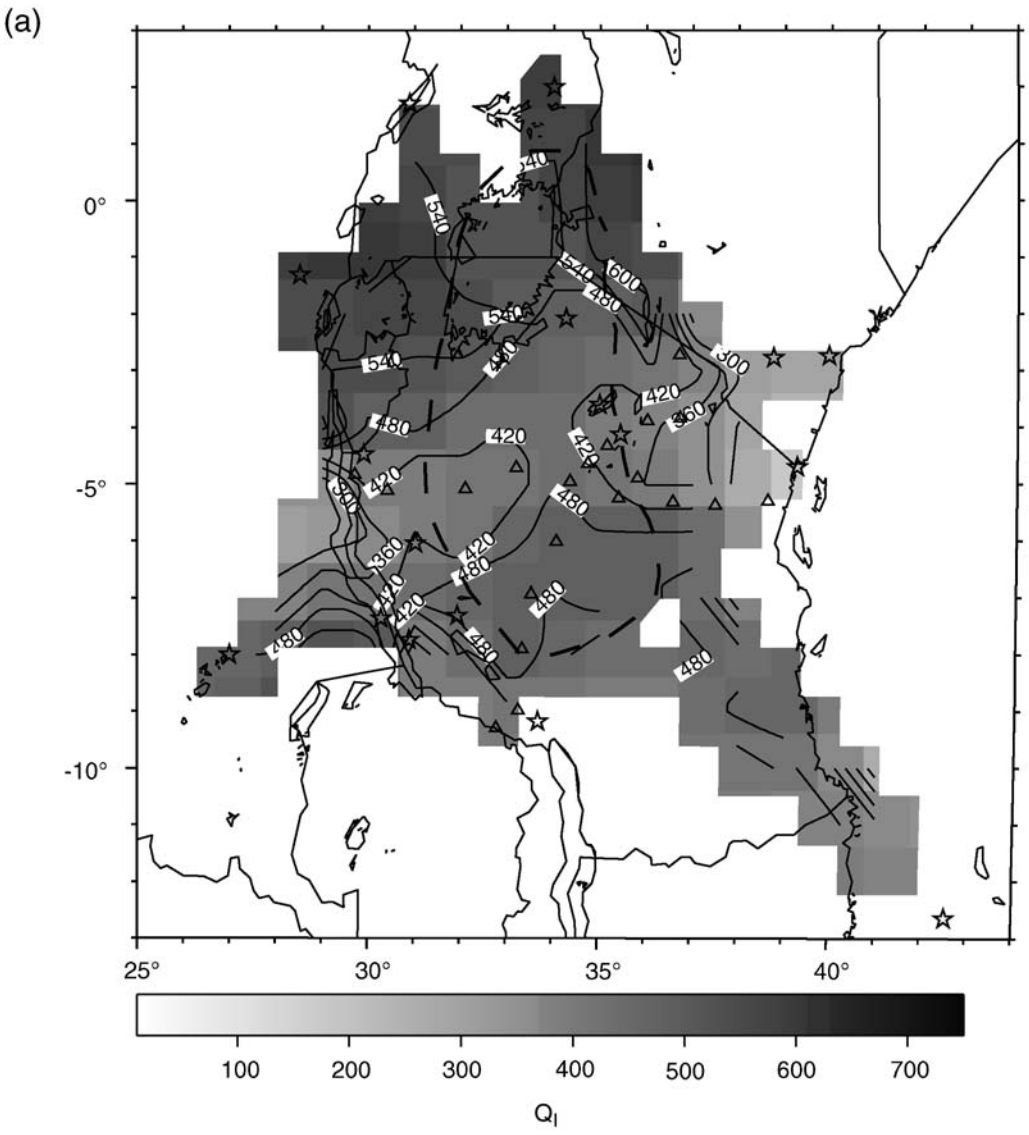

Figure 3. (a) Lateral variation of 1 Hz intrinsic Q (Q_I) across the Tanzania craton and the adjacent mobile belts. Event and stations locations are the same as in Figure 1a. The bold dashed line shows the location of the Tanzania craton. (b) Lateral variation of 1 Hz scattering Q (Q_S) across the Tanzania craton and the adjacent mobile belts. Event and stations locations are the same as in Figure 1a. The bold dashed line shows the location of the Tanzania craton. (*Continued*)

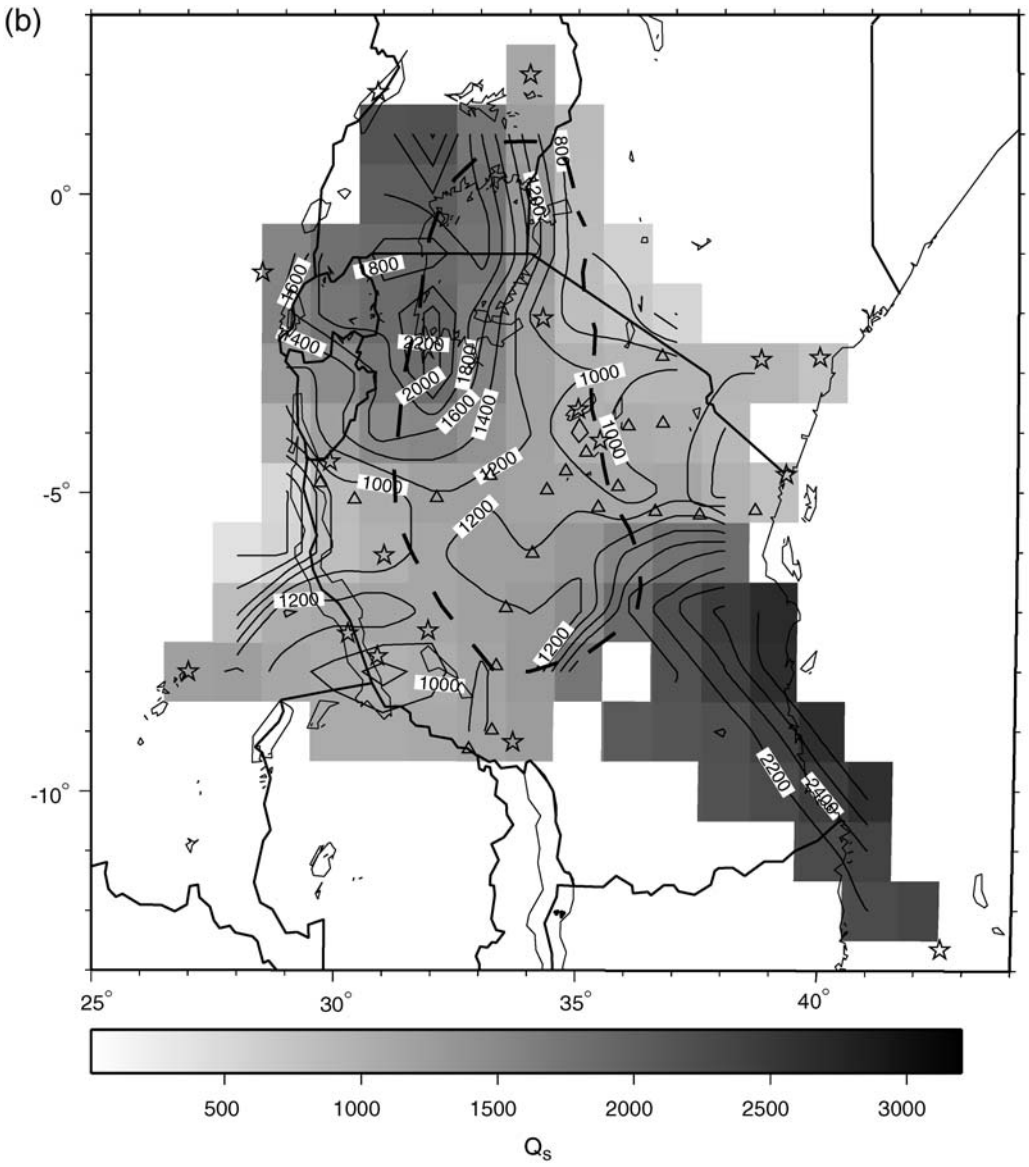

Figure 3. Continued.

mobile belts. Interestingly, Q_I does not diminish appreciably along the eastern margin of the Tanzania craton where the eastern branch of the rift system has fractured the cratonic crust in a series of block faults. Q_S ranges from ~1000 in the mobile belts surrounding the craton and eastern margin of the Tanzania craton to ~2200 in the northwestern side of the Tanzania craton just south of Lake Victoria.

Our estimates of intrinsic and scattering Q values are the first such estimates for crust in East Africa, and also the first for rifted Precambrian crust anywhere. Because of this, interpreting them via a comparison to published Q_I and Q_S for similar terrains is not possible. However, Mitchell (1995) noted that Q values determined from direct 1 Hz *Lg* waves are usually similar to Q values determined from 1 Hz *Lg* coda. He also concluded that crustal Q estimated from *Lg* or its coda is governed primarily by intrinsic rather than scattering attenuation mechanisms. Therefore, to interpret our results *vis-á-vis* factors that can influence crustal Q, we first compare our estimates of Q_I to Q values obtained from 1 Hz *Lg* or its coda for different regions by other investigators (Table 2).

From the Q values in Table 2, it can be seen that there is a fairly large range in Q estimates for Precambrian crust, ranging from a low of 157 to a high of 1000. Most of the regions, however, have Q values for 500 or more. Thus, it appears that the Q_I estimates of ~300 to 600 for Tanzania fall within the lower part of the global Precambrian crustal Q distribution, with the midrange Q_I value for Tanzania about 30%–50% lower than the midrange crustal Q value for most Precambrian terrains.

Given the Cenozoic rifting and volcanism that has affected much of East Africa, a reasonable assumption would

Table 2

Q from 1 Hz *Lg* or Its Coda for Precambrian Terrains

Continent	Region	*Q* from 1 Hz *Lg* Coda	*Q* from 1 Hz *Lg*	Reference
Africa	Tanzania craton	360 to ~500		Mitchell, 1995; Romanowicz and Mitchell, 2007
	Congo craton	460 to 760		
	Kalahari craton	560 to 860		
	West African craton	860 to 960		
	East Sahara craton	860 to 960		
Middle East	Arabian peninsula	157 to 300		Mitchell, 1995
		300 to 450		Romanowicz and Mitchell, 2007; Mitchell, *et al.*, 2008
	Northern Arabian platform		~250 to 350	Zor *et al.*, 2007
	Southern Arabian plate		~670 to 800	Zor *et al.*, 2007
Australia	Central Australia	~230		Mitchell, 1995
	Yilgarn and Gawler blocks	550 to 600		Romanowicz and Mitchell, 2007
	Much of remaining cratonic crust	400 to 500		
Eurasia	Siberian craton	400 to 600		Mitchell, 1995
	Western portion of Siberian craton	300 to 500		Mitchell, *et al.*, 2008
	Indian shield	600 to 950		Romanowicz and Mitchell, 2007
			665	Mitra *et al.*, 2006
North America	Superior and Greenville provinces; Canadian shield	650 to 800		Romanowicz and Mitchell, 2007
	Superior province; Canadian shield	730		Woodgold, 1990
	Greenville province; Canadian shield	600 to 770		
South America	Guyana shield; Brazilian shield	700 to 1000		Romanowicz and Mitchell, 2007

be that the lower Q for the Tanzania crust arises from elevated crustal temperatures. However, heat flow measurements from the Tanzania craton and surrounding mobile belts (Fig. 1) are not elevated (Nyblade *et al.*, 1990; Nyblade, 1997), and consequently invoking elevated crustal temperatures to explain the lower Q_I estimates cannot be justified. In fact, heat flow from the Tanzania craton and the surrounding mobile belts is on average about 5–10 mW m^{-2} lower than the global averages for Archean cratons and Proterozoic mobile belts (Nyblade, 1997); therefore, if anything, one would expect the Q_I estimates to be higher than average, not lower.

An alternative explanation for the lower than average Q_I estimates for the crust in Tanzania is that many fractures in the upper crust, which have resulted from the rift faulting, are interconnected and filled with fluids. This is a plausible explanation given the morphology of the rift system in Tanzania (Fig. 1), and we favor it over an interpretation invoking elevated crustal temperatures. As noted in the Background section, the eastern branch of the rift system developed within the Mozambique belt and the eastern margin of the craton, with rift faults extending 100 to 200 km into the interior of the craton. On the western side of the craton numerous faults within the western branch of the rift system have fractured the upper crust of the Kibaran and Ubendian belts. In total, crust covering roughly two-thirds of the study area has been affected by rift faulting, likely creating an extensive fracture network that affects *Lg* waves propagating across the East African plateau.

Scattering Q (Q_S) is two to four times greater than Q_I throughout much of the Tanzania craton and the surrounding mobile belts (Figs. 3a,b). This difference is consistent with previous studies where both Q_S than Q_I values are available (Langston, 1989; Wennerberg, 1993). In comparing our Q_S and Q_I estimates to the Q values of 360–500 reported for the Tanzania craton by Mitchell (1995) using 1 Hz *Lg* coda, it is apparent that overall intrinsic attenuation mechanisms dominate over scattering mechanisms throughout the study region. This finding is consistent with the conclusion reached by Mitchell (1995) for other parts of the world.

The high values of Q_S (~1000–2200) found across the study area indicate that the plateau crust has not been affected to any great extent by the Cenozoic rifting in terms of creating large basins, rift flank mountain ranges, or regions with a shallow Moho. As noted previously, upper crust has been fractured by rift faults in some places, but the rift basins bounded by those faults are small and shallow, and overall the structure of the crust has remained largely intact (see review of crustal structure in the Background section).

Differences of up to 1000 in Q_S can be seen in Figure 3b, with the highest values in the interior of the East African plateau at the southwest end of Lake Victoria. This variability in Q_S is most easily attributable to scattering of *Lg* by surface topography and heterogeneous upper crustal structure, in particular narrow and shallow rift basins. Because of the rift faulting in the mobile belts surrounding the craton and also along the eastern margin of the craton, the topography in

the middle of the plateau is more subdued than along the sides of the plateau.

Summary

We have investigated crustal attenuation across the middle of the East African plateau in Tanzania, an area of Precambrian crust that has been affected by Cenozoic rift faulting. By using 1 Hz *Lg* coda waves and the energy flux model of Frankel and Wennerberg (1987), we provide the first estimates of Q_I and Q_S for East Africa. Q_I values over the study area are fairly uniform, ranging from a low of ~300 to a high of ~600. Similar values of Q_I are found in both the Tanzania craton and the surrounding mobile belts. Interestingly, Q_I does not diminish appreciably along the eastern margin of the Tanzania craton where the eastern branch of the rift systems has fractured the cratonic crust in a series of block faults. The Q_I estimates for the crust in Tanzania are somewhat lower than the average Q values for Precambrian crust elsewhere. Heat flow from the Tanzania craton and surrounding mobile belts is not elevated; therefore, we attributed the lower-than-average Q values to fractures in the upper crust formed by the Cenozoic rifting that are interconnected and filled with fluids.

Q_S ranges from ~1000 in the mobile belts surrounding the craton and eastern margin of the Tanzania craton to ~2200 in the northwestern side of the Tanzania craton just south of Lake Victoria. The variability in Q_S is most easily attributable to scattering of *Lg* by surface topography and heterogeneous upper crustal structure, in particular rift basins along the eastern side of the plateau. Because of the rift faulting in the mobile belts surrounding the craton and also along the eastern margin of the craton, the topography in the middle of the plateau is more subdued than along the sides of the plateau.

Data and Resources

Data from the 1994–1995 Tanzania broadband seismic experiment are available to the public at www.iris.edu/data/.

Acknowledgments

Alemayehu Jemberie acknowledges support from AfricaArray (www.africaarray.psu.edu), North Carolina A&T State University, and Solomon Bililign while working on this article. Funding for this research has been provided by NSF (grants OISE 0530062 and EAR 9304555).

References

Aki, K. (1969). Analysis of the seismic coda of local earthquakes as scattered waves, *J. Geophys. Res.* **74,** 615–631.

Baumont, D., A. Paul, S. Beck, and G. Zandt (1999). Strong crustal heterogeneity in the Bolivian Altiplano as suggested by attenuation of *Lg* waves, *J. Geophys. Res.* **104,** 20,287–20,305.

Bonjer, K. P., K. Fuchs, and J. Wohlenburg (1970). Crustal structure of the East African rift system from spectral response ratios of long period body waves, *Z. Geophys.* **36,** 287–297.

Bram, K., and B. D. Schmeling (1975). Structure of the crust and upper mantle beneath the western rift of East Africa, derived from investigations of near earthquakes, in *Afar Between Continental and Oceanic Rifting*, A. Pilger and A. Rosier (Editors), Schweizerbart, Stuttgart, Germany, 138–142.

Dugda, M. T., A. A. Nyblade, J. Julia, C. A. Langston, C. J. Ammon, and S. Simiyu (2005). Crustal structure in Ethiopia and Kenya from receiver function analysis: Implications for rift development in eastern Africa, *J. Geophys. Res.* **110,** B01303, doi 10.1029/2004JB003065.

Fan, G.-W., and T. Lay (2003). Strong L_g attenuation in the Tibetan plateau, *Bull. Seismol. Soc. Am.* **93,** 2264–2272.

Farnbach, J. S. (1975). The complex envelope in seismic signal analysis, *Bull. Seismol. Soc. Am.* **65,** 951–962.

Frankel, A. (1991). Mechanisms of seismic attenuation in the crust: Scattering and anelasticity in New York State, South Africa, and Southern California, *J. Geophys. Res.* **96,** no. B4, 6269–6289.

Frankel, A., and L. Wennerberg (1987). Energy-flux model of seismic coda: Separation of scattering and intrinsic attenuation, *Bull. Seismol. Soc. Am.* **77,** 1223–1251.

Frankel, A., A. McGarr, J. Bicknell, J. Mori, L. Seeber, and E. Cranswick (1990). Attenuation of high-frequency shear waves in the crust: Measurements from New York State, South Africa, and Southern California, *J. Geophys. Res.* **95,** no. B11, 17,441–17,457.

Fuchs, K., R. Altherr, B. Muller, and C. Prodehl (Editors) (1997). Structure and dynamic processes in the lithosphere of the Afro-Arabian rift system, *Tectonophysics* **278,** special issue, 352 pp.

Griffiths, D., R. King, M. Khan, and D. Blundell (1971). Seismic refraction line in the Gregory rift, *Nature* **229,** 69–71.

Hauksson, E., and P. M. Shearer (2006). Attenuation models (Q_p and Q_s) in three dimensions of the southern California crust: Inferred fluid saturation at seismogenic depths, *J. Geophys. Res.* **111,** B05302, doi 10.1029/2005JB003947.

Hebert, L., and C. A. Langston (1985). Crustal thickness estimate at AAE (Addis Ababa, Ethiopia) and NAI (Nairobi, Kenya) using teleseismic *P*-wave conversions, *Tectonophysics* **111,** 299–327.

Jemberie, A. L., and C. A. Langston (2005). Site amplification, scattering, and intrinsic attenuation in the Mississippi embayment from coda waves, *Bull. Seismol. Soc. Am.* **95,** 1716–1730.

Jemberie, A. L., and B. J. Mitchell (2004). Shear-wave Q structure and its lateral variation in the crust of China and surrounding regions, *Geophys. J. Int.* **157,** 363–380.

Julia, J., C. J. Ammon, and A. A. Nyblade (2005). Evidence for mafic lower crust in Tanzania, East Africa, from joint inversion of receiver functions and Rayleigh wave dispersion velocities, *Geophys. J. Int.* **162,** 555–569.

Kennett, B. L. N. (1986). *Lg* waves and structural boundaries, *Bull. Seismol. Soc. Am.* **76,** 1133–1141.

Langston, C. (1989). Scattering of teleseismic body waves under Pasadena, California, *J. Geophys. Res.* **94,** no. B2, 1935–1951.

Langston, C. A., R. Brazier, A. A. Nyblade, and T. J. Owens (1998). Local magnitude scale and seismicity rate for Tanzania, East Africa, *Bull. Seismol. Soc. Am.* **88,** 712–721.

Langston, C. A., A. A. Nyblade, and T. J. Owens (2002). Regional wave propagation in Tanzania, East Africa, *J. Geophys. Res.* **107,** no. B1, 2003, doi 10.1029/2001JB000167.

Last, R., A. Nyblade, C. Langston, and T. Owens (1997). Crustal structure of the East African plateau from receiver functions and Rayleigh wave phase velocities, *J. Geophys. Res.* **102,** no. B11, 24,469–24,483.

Long, R. E., R. W. Backhouse, P. K. H. Maguire, and K. Sundarlingham (1972). The structure of East Africa using the surface wave dispersion and Durham seismic array data, *Tectonophysics* **15,** 165–178.

Mayeda, K., L. Malagnini, W. S. Phillips, W. R. Walter, and D. Dreger (2005). 2-D or not 2-D, that is the question: A northern California test, *Geophys. Res. Lett.* **32,** L12301, doi 10.1029/2005GL022882.

Mitchell, B. (1995). Anelastic structure and evolution of the continental crust and upper mantle from seismic surface wave attenuation, *Rev. Geophys.* **33,** no. 4, 441–462.

Mitchell, B., L. Cong, and G. Ekström (2008). A continent-wide map of 1-Hz *Lg* coda *Q* variation across Eurasia and its relation to lithospheric evolution, *J. Geophys. Res.* **113,** B04303, doi 10.1029/2007JB005065.

Mitra, S. K. Priestley, V. K. Gaur, and S. S. Rai (2006). Frequency-dependent *Lg* attenuation in the Indian platform, *Bull. Seismol. Soc. Am.* **96,** 2449–2456.

Morasca, P., K. Mayeda, R. Gok, S. Phillips, and L. Malagnini (2008). 2D coda and direct-wave attenuation tomography in northern Italy, *Bull. Seismol. Soc. Am.* **98,** 1936–1946.

Mueller, S., and K. P. Bonjer (1973). Average structure of the crust and upper mantle in East Africa, *Tectonophysics* **20,** 238–253.

Nolet, G., and St. Mueller (1982). A model for the deep structure of the East African rift system from simultaneous inversion of teleseismic data, *Tectonophysics* **84,** 151–178.

Nyblade, A. (1997). Heat flow across the East African plateau, *Geophys. Res. Lett.* **24,** no. 16, 2083–2086.

Nyblade, A. A., C. Birt, C. A. Langston, T. J. Owens, and R. Last (1996). Seismic experiment reveals rifting of craton in Tanzania, *Eos Trans. AGU* **77,** 517–521.

Nyblade, A., H. Pollack, D. Jones, F. Podmore, and M. Mushayandebvu (1990). Terrestrial heat flow in East and Southern Africa, *J. Geophys. Res.* **95,** no. B11, 17,371–17,384.

O'Connell, R. J., and B. Budiansky (1977). Viscoelastic properties of fluid-saturated cracked solids, *J. Geophys. Res.* **82,** 5719–5735.

Press, F., and M. Ewing (1952). Two slow surface waves across North America, *Bull. Seismol. Soc. Am.* **42,** 219–228.

Prodehl, C., G. R. Keller, and M. A. Khan (Editors) (1994). Crustal and upper mantle structure of the Kenya rift, *Tectonophysics* **236,** special issue, 483 pp.

Romanowicz, B., and B. J. Mitchell (2007). Deep earth structure—*Q* of the Earth from crust to core, in *Seismology and the Structure of the Earth*, Barbara Romanowicz and Adam Dziewonski (Editors), of *Treatise on Geophysics*, Gerald Schubert (Editor-in-Chief), Vol. **1**, Elsevier, Amsterdam, 737–774.

Rudnick, R. L., and S. Gao (2004). Composition of the continental crust, in *Treatise on Geochemistry*, H. D. Holland and K. K. Turekian (Editors), Elsevier, Amsterdam, **3,** 1–64.

Sarker, G., and G. A. Abers (1999). Lithospheric temperature estimates from seismic attenuation across range fronts in southern and central Eurasia, *Geology* **27,** 427–430.

Sato, H. (1977). Energy propagation including scattering effects; single isotropic scattering, *J. Phys. Earth* **25,** 27–41.

Wennerberg, L. (1993). Multiple-scattering interpretations of coda-*Q* measurements, *Bull. Seismol. Soc. Am.* **83,** 279–290.

Wessel, P., and W. H. F. Smith (1998). New, improved version of generic mapping tools released, *Eos Trans. AGU* **79,** no. 47, 579.

Woodgold, C. R. D. (1990). Estimation of *Q* in eastern Canada using coda waves, *Bull. Seismol. Soc. Am.* **80,** 411–429.

Xie, J., R. Gok, J. Ni, and Y. Aoki (2004). Lateral variations of crustal seismic attenuation along the INDEPTH profiles in Tibet from *Lg Q* inversion, *J. Geophys. Res.* **109,** B10308, doi 10.1029/2004JB002988.

Zor, E., E. Sandvol, J. Xie, N. Turkelli, B. Mitchell, A. H. Gasanov, and G. Yetirmishli (2007). Crustal attenuation within the Turkish plateau and surrounding regions, *Bull. Seismol. Soc. Am.* **97,** no. 1B, 151–161.

Impact Forecasting
AonBenfield, 200 East Randolph Street
15th floor, Chicago, Illinois 60601
Alemayehu_Jemberie@aonbenfield.com
(A.L.J.)

The Department of Geosciences
Pennsylvania State University
University Park, Pennsylvania 16802
andy@geosc.psu.edu
(A.A.N.)

Manuscript received 5 March 2009